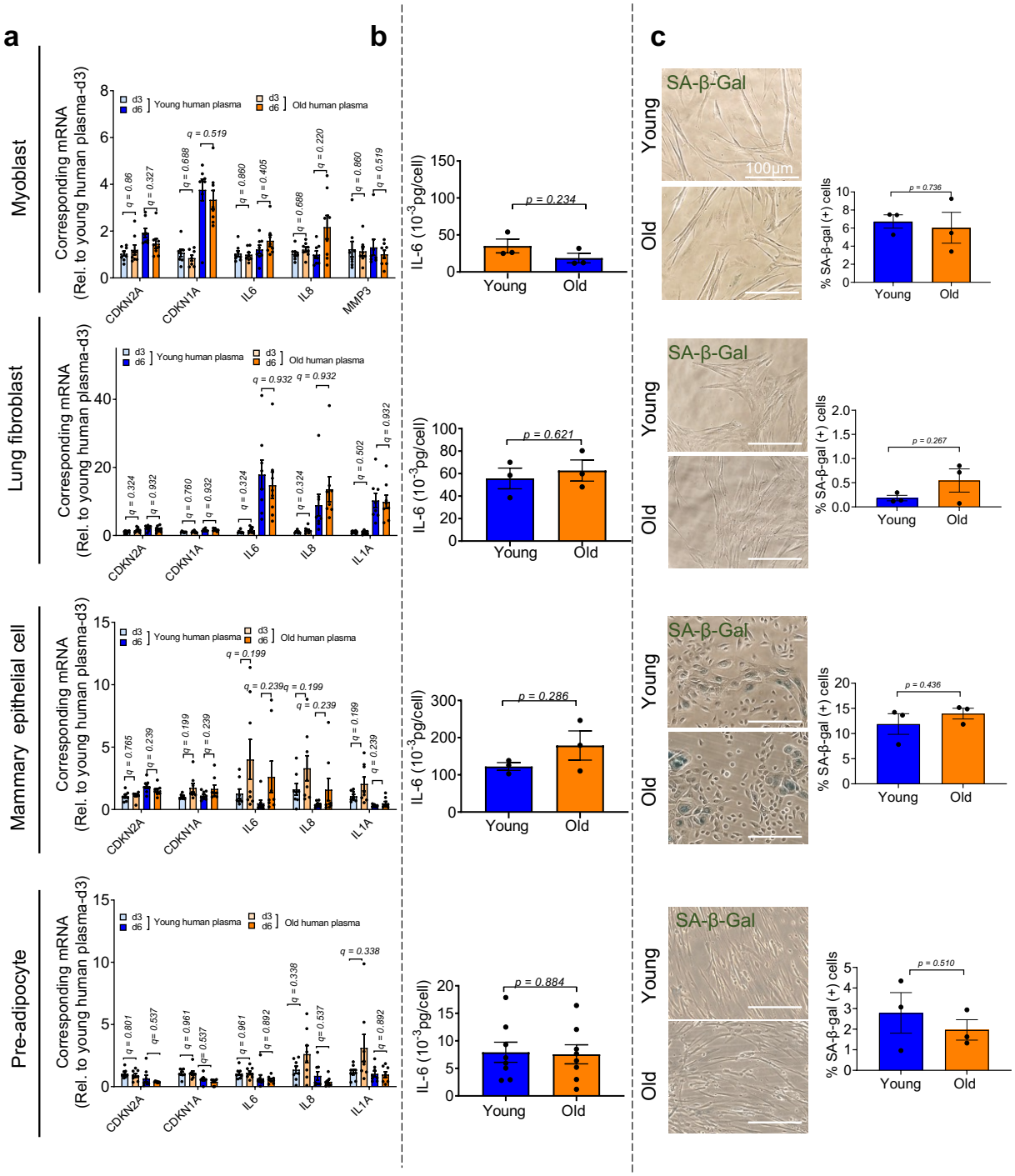
a
b
c
Myoblast
Lung fibroblast
Mammary epithelial cell
Pre-adipocyte
Corresponding mRNA (Rel. to young human plasma-d3)
d3
d6
Young human plasma
Old human plasma
CDKN2A
CDKN1A
IL6
IL8
MMP3
IL1A
IL-6 (10-3pg/cell)
p = 0.234
p = 0.621
p = 0.286
p = 0.884
Young
Old
SA-β-Gal
100μm
% SA-β-gal (+) cells
p = 0.736
p = 0.267
p = 0.436
p = 0.510

Supplementary Fig 1. Old human plasma induces cell senescence in culture, which but is cell and tissue-specific response. (a) Expression of the senescence and SASPs marker panel, as determined by RT–PCR in human skeletal muscle myoblasts, lung fibroblast, mammary epithelial cells, and pre-adipocytes by culturing with young (20 years old) or old (70 years old) human plasma for 3 or 6 days (d3 or d6). (b) The level of IL-6 secreted by, and (c) representative SA-β-gal staining (left; green) and quantification of the percentage of SA-β-gal-positive cells in, different cells treated in young or human plasma for 6 days (n = 3 per group / 3-6 images per n). Scale bars, 100 μm. Data are means ± s.e.m. of biologically independent samples. Statistical significance was calculated using multiple two-tailed t test with a two-stage linear step-up procedure of Benjamini, Krieger and Yekutieli, with Q = 5%, *q < 0.05 (a) and unpaired two-tailed t test with a Welch's correction (b-c).

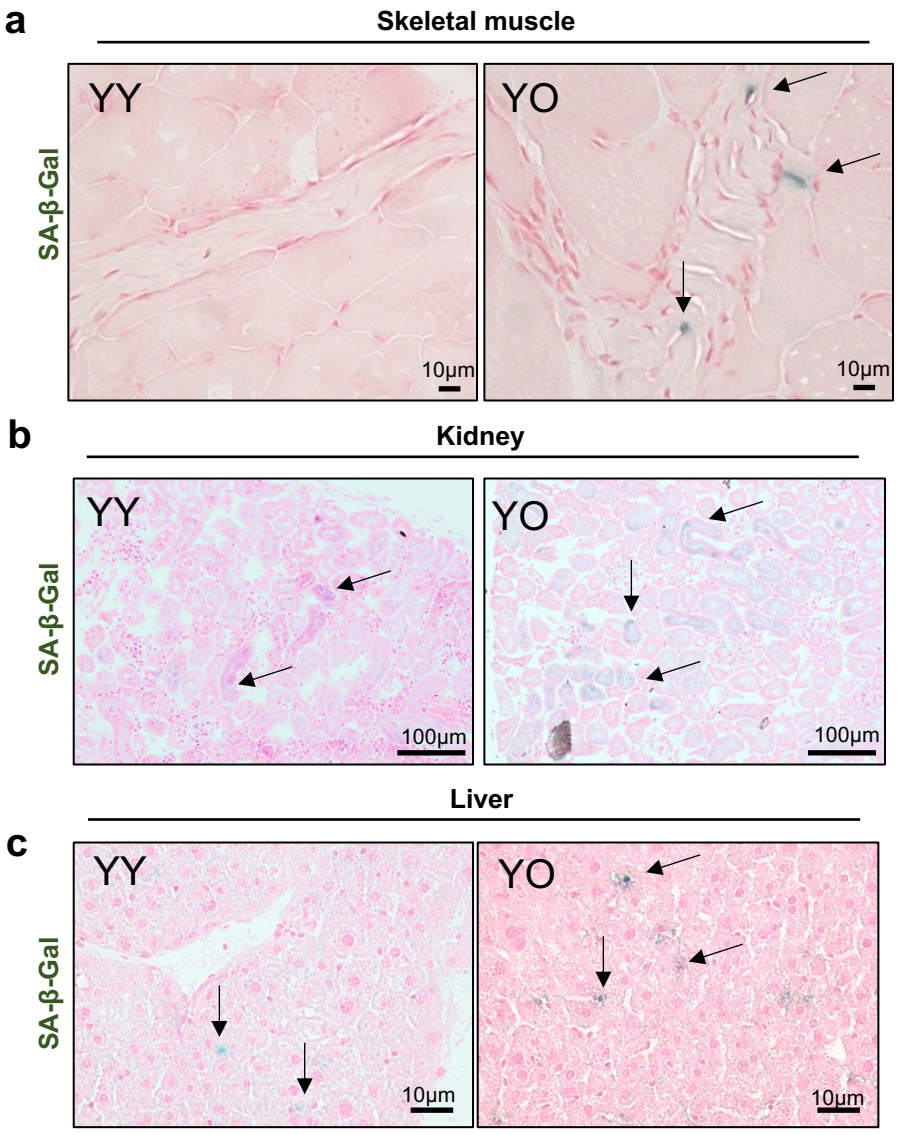

Supplementary Fig 2. An aging systemic milieu induces senescence transfer in young kidney and liver tissues. Additional SA-β gal images of (a) skeletal muscle (n = 4 mice for YY and n = 5 mice for YO ; 3-6 images per mice), (b) kidney (n = 8 mice for YY or YO / 7-10 images per mice) and (c) liver (*n* = 9 mice for YY; *n* = 8 mice for YO; 7-10 images per mice) in young male p16-3MR mice receiving young blood from C57BL/6J mice (YY) and young p16-3MR mice receiving old blood from C57BL/6J mice (YO) 14 days after heterochronic blood exchange.

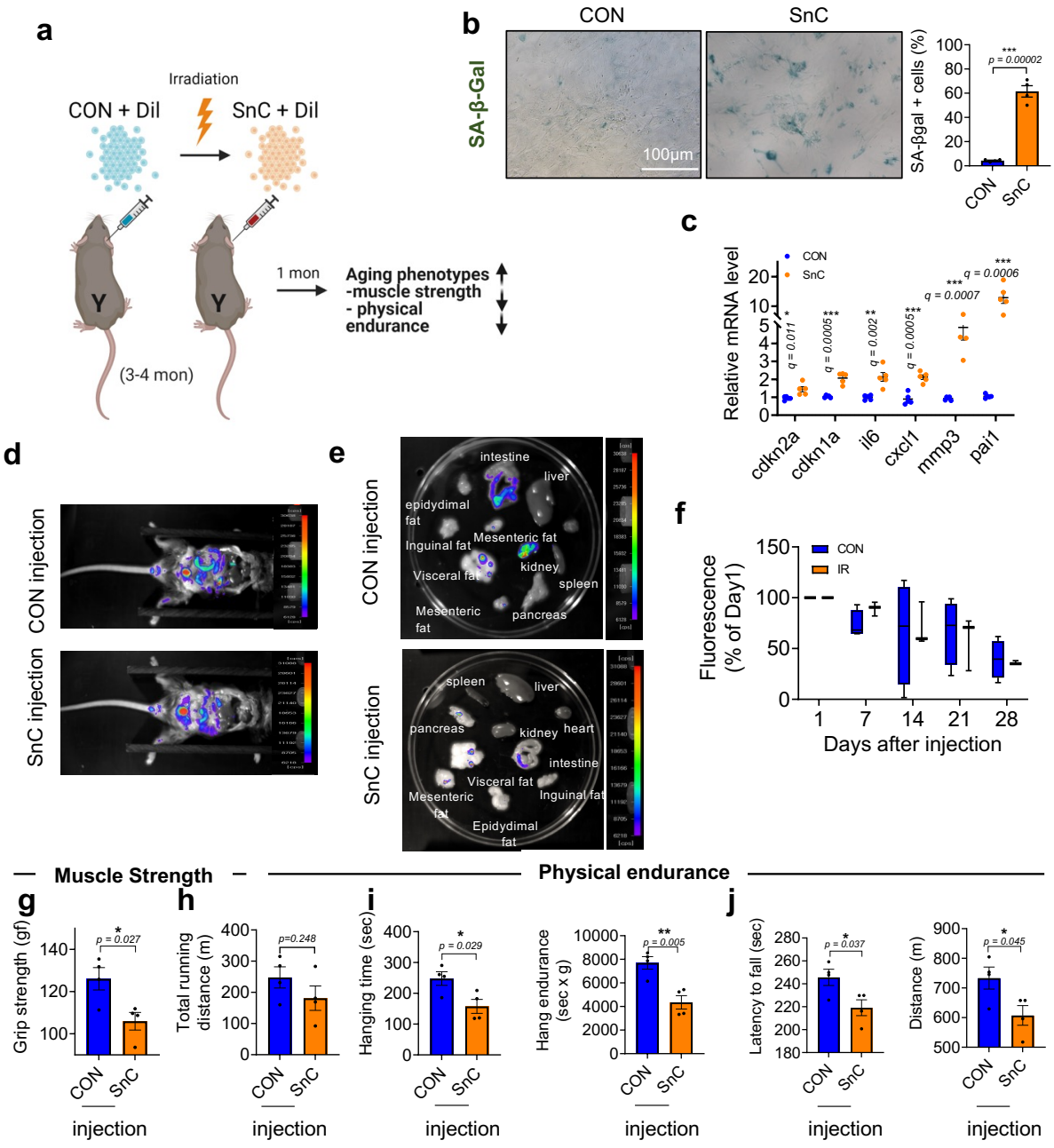
a
Irradiation
CON + DiI
SnC + DiI
Y
Y
(3-4 mon)
1 mon
Aging phenotypes
-muscle strength
- physical
endurance
b
CON
SnC
SA-β-Gal
100μm
SA-βgal + cells (%)
p = 0.00002
c
CON
SnC
Relative mRNA level
q = 0.011
q = 0.0005
q = 0.002
q = 0.0005
q = 0.0007
q = 0.0006
cdkn2a
cdkn1a
il6
cxcl1
mmp3
pai1
d
CON injection
SnC injection
e
CON injection
intestine
liver
epididymal fat
Mesenteric fat
Inguinal fat
Visceral fat
kidney
spleen
Mesenteric fat
pancreas
SnC injection
spleen
liver
pancreas
kidney
heart
intestine
Visceral fat
Mesenteric fat
Inguinal fat
Epididymal fat
f
CON
IR
Fluorescence (% of Day1)
Days after injection
Muscle Strength
Physical endurance
g
Grip strength (gf)
p = 0.027
CON
SnC
injection
h
Total running distance (m)
p=0.248
CON
SnC
injection
i
Hanging time (sec)
p = 0.029
CON
SnC
injection
Hang endurance (sec x g)
p = 0.005
CON
SnC
injection
j
Latency to fall (sec)
p = 0.037
CON
SnC
injection
Distance (m)
p = 0.045
CON
SnC
injection

Supplementary Fig 3. Exogeneous delivery of SnCs induce aging phenotypes in young mice. (a) Schematic of experiment. 3-4-month-old C57BL/6J mice were injected intraperitoneally (i.p.) with senescent (SnC) or non-senescent (CON) mouse pre-adipocytes, labelled with Dil from C57BL/6J mice. (b) Representative images of SA-β-gal staining of SnC (induced by irradiation) and CON primary mouse preadipocytes (n = 5 for each group / 5 images per n). Scale bars, 100 μm. (c) Relative mRNA levels of senescence and SASP markers of SnC and CON primary mouse preadipocytes (n = 5 for each group). (d) Representative fluorescence images of mice 5 days after SnC and CON injection (n = 4 mice for CON injection; n = 3 mice for SnC injection). (e) Fluorescence of various organs 5 days after exogeneous delivery of SnCs. (f) Fluorescence of mice at different times after transplantation. In the-whisker plot, whiskers represent the 10 and 90 percentiles and the line corresponds to the median (n = 4 for CON injection; n = 3 for SnC injection). Grip strength (g), treadmill running distance (h), hang time and endurance (i), and latency time to fall from the rotarod apparatus and distance before fall (j) in young mice one month after SnC or CON injection. Data are collective of two (b, c) and one (d-j) independent experiment. Data are means ± s.e.m. of biologically independent samples. Statistical significance was calculated using two-tailed Student's t test (b, g-j) with *, $P < 0.05$; **, $P < 0.01$; ***, $P < 0.001$ and multiple t-tests with a two-stage linear step-up procedure of Benjamini, Krieger and Yekutieli, with Q = 5%, *$q < 0.05$; **$q < 0.01$; ***$q < 0.001$ (c).

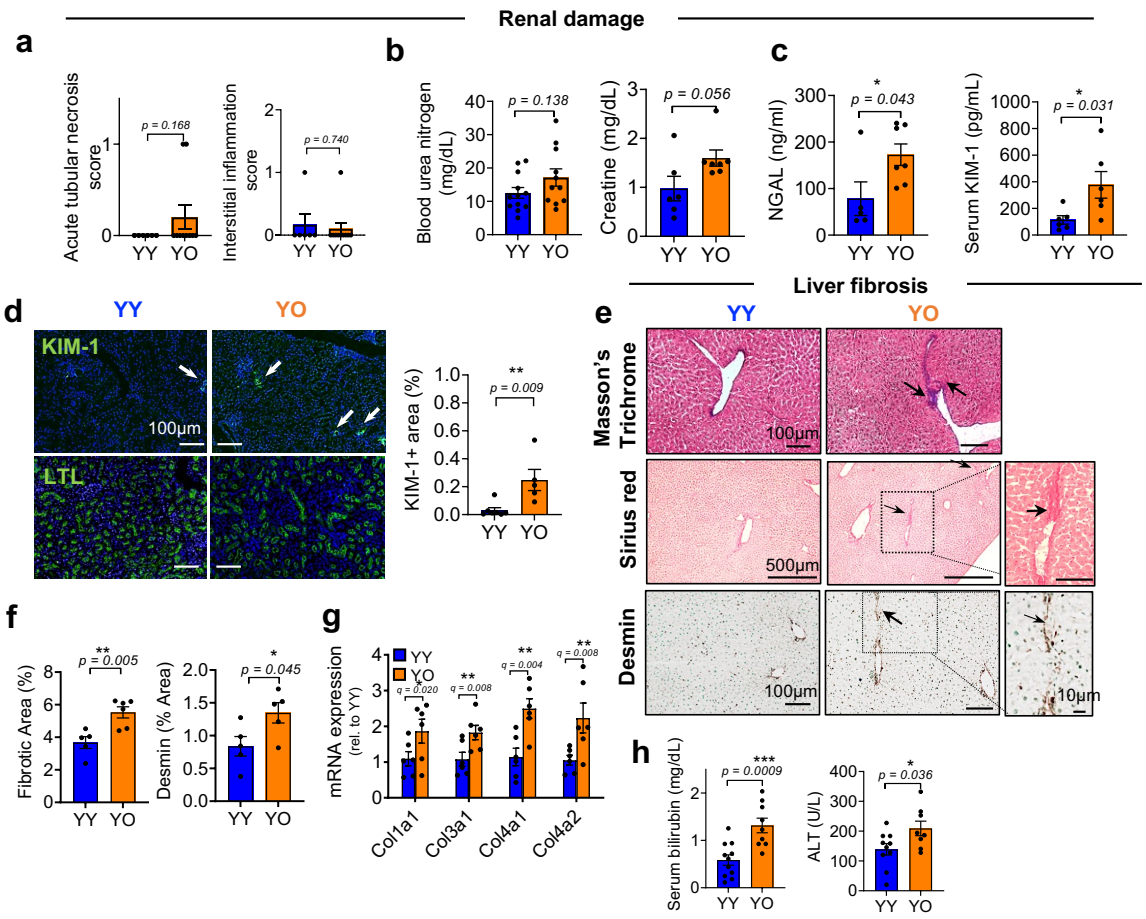

Supplementary Fig 4. Aged blood increases renal damage in young mice and confers hepatic damage and fibrosis to young liver. (a) Scores of acute tubular necrosis and interstitial inflammation in the renal cortex ($n = 6$ for YY; $n = 10$ for YO). Measurements of (b) blood urea nitrogen ($n = 12$ for YY; $n = 11$ for YO) and creatine ($n = 6$ for YY; $n = 7$ for YO), (c) neutrophil gelatinase-associated lipocalin (NGAL) ($n = 5$ for YY; $n = 7$ for YO) and KIM-1 levels ($n = 6$ for each group). (d) Immunohistochemical staining for KIM-1 and Lotus Tetragonolobus Lectins (LTL), which combines tubular brush borders with specific coloring at the proximal end as a marker for healthy renal tubules (left) and quantification of KIM-1 positive area (%) (right) ($n = 7$ for YY; $n = 5$ for YO; 4-6 images per mice). (e) Representative images of Masson's trichrome ($n = 6$ mice for YY; $n = 4$ mice for YO; 9-13 images per mice) and Sirius red staining and desmin immunohistochemistry in liver. % of desmin-positive areas. (f) Quantification of collagen deposition, as the % of area occupied by Sirius Red stain (left; $n = 5$ for YY; $n = 6$ for YO; 8-10 images per mice) and % of desmin-positive areas (right; $n = 5$ per group/6-10 images per mice). (g) Quantification of mRNA levels for *Col1a1, Col3a1, Col4a1* and *Col4a2* in the liver ($n = 6$ per group). (h) Serum analysis of bilirubin ($n = 11$ for YY; $n = 9$ for YO) and ALT ($n = 10$ for YY; $n = 8$ for YO) showed old blood induced hepatocyte injury in young mice, although these markers are not indicators of hepatic failure per se. Data are means ± s.e.m. of biologically independent samples. A two-tailed *t* test with a Welch's correction (a) and Student *t*-test (b-d, f, h), with *, $P < 0.05$; **, $P < 0.01$; ***, $P < 0.001$ and multiple *t*-tests with a two-stage linear step-up procedure of Benjamini, Krieger and Yekutieli, with Q = 5%, *$q < 0.05$; **$q < 0.01$ (g) were used for statistical analysis. Scale bars are shown in each image.

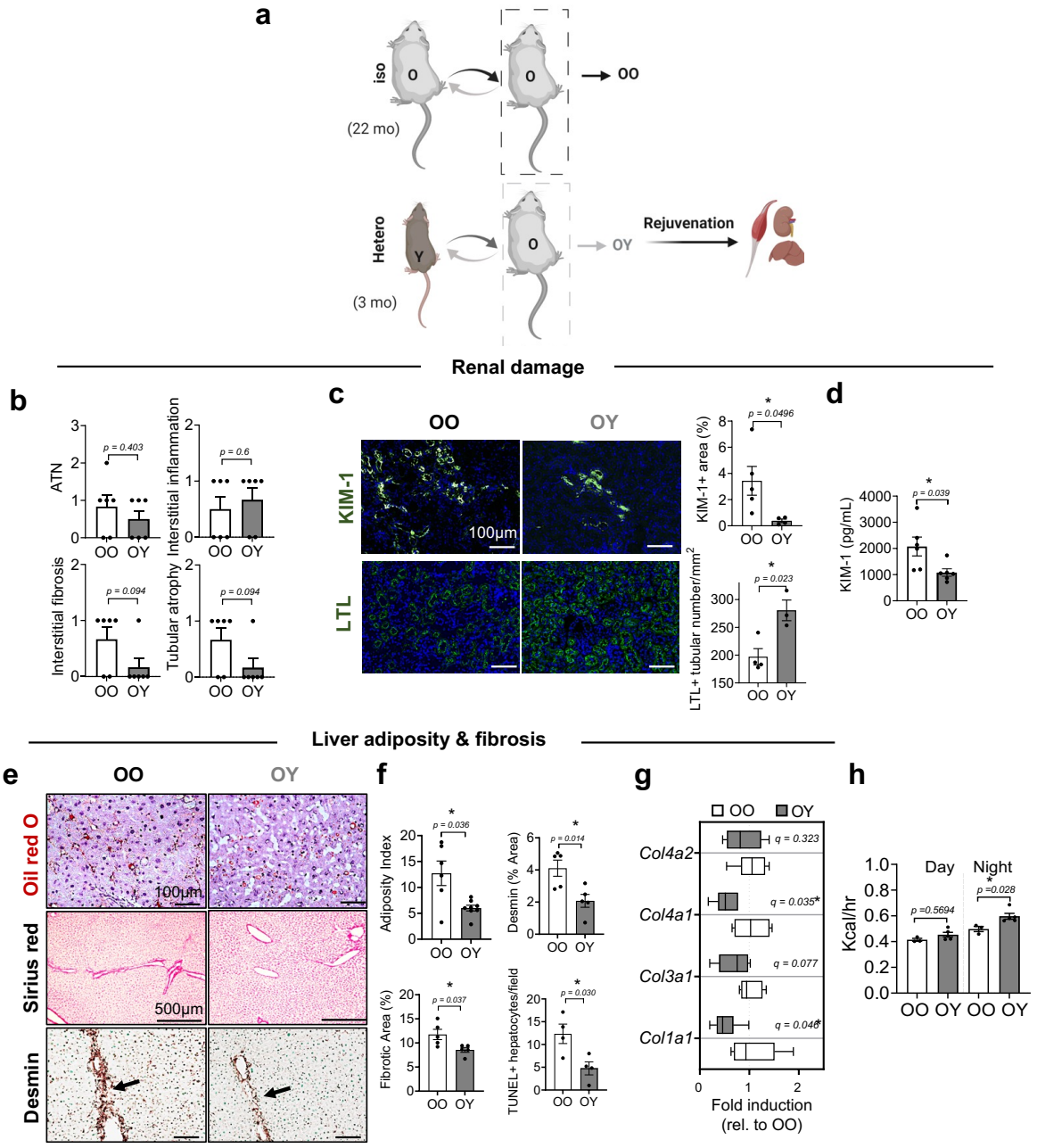
a
iso
(22 mo)
OO
Hetero
(3 mo)
OY
Rejuvenation
Renal damage
b
ATN
Interstitial inflammation
Interstitial fibrosis
Tubular atrophy
p = 0.403
p = 0.6
p = 0.094
p = 0.094
OO OY
c
OO
OY
KIM-1
LTL
100μm
KIM-1+ area (%)
p = 0.0496
LTL+ tubular number/mm2
p = 0.023
d
KIM-1 (pg/mL)
p = 0.039
Liver adiposity & fibrosis
e
Oil red O
Sirius red
Desmin
100μm
500μm
f
Adiposity Index
p = 0.036
Desmin (% Area)
p = 0.014
Fibrotic Area (%)
p = 0.037
TUNEL+ hepatocytes/field
p = 0.030
g
Col4a2
Col4a1
Col3a1
Col1a1
q = 0.323
q = 0.035*
q = 0.077
q = 0.046*
Fold induction
(rel. to OO)
h
Kcal/hr
Day
Night
p =0.5694
p =0.028
OO OY OO OY

Supplementary Fig 5. Young blood effects on old mouse renal and liver function after heterochronic blood exchange. (a) Experimental setup. (b) Scores of acute tubular necrosis (ATN), interstitial inflammation, interstitial fibrosis and tubular atrophy of renal cortex of old mice receiving old blood (OO) and old mice receiving young blood (OY) mice 14 days after blood exchange (n = 6 per group). (c) Representative images of KIM-1 and LTL by immunofluorescence in kidneys (left) and quantification of KIM-1 + area (%; n = 5 for OO; n = 4 for OY; 5-7 images per mice) and LTL+ healthy tubular numbers (n = 4 for OO; n = 3 for OY; 5-6 images per mice) (right). (d) Measurements of KIM-1 levels (n = 6 per group). (e) Oil Red O staining to assay liver adiposity (n = 6 for OO; n = 8 for OY; 7-10 images per mice). Sirius red staining and immunohistochemistry for desmin (n = 5 mice per group/10-13 images per mice). (f) Liver adiposity (n = 6 for OO; n = 8 for OY), fibrotic area (n = 5 per group), desmin + areas and TUNEL+ hepatocytes (n = 4 mice per group/3 images per mice). (g) Quantification of mRNA levels encoding *Col1a1, Col3a1, Col4a1* and *Col4a2* in the liver. In the-whisker plot, whiskers represent the 10 and 90 percentiles and the line corresponds to the median (n = 6 per group). (h) Measured energy expenditure of OO and OY mice during the day and night cycles in metabolic cages (n = 3 for OO; n = 5 for OY). Data are the average of 4 day and night cycles for 4 consecutive days. Data are means ± s.e.m. of biologically independent samples. A two-tailed t test with a Welch's correction (b-d, f; *, $P < 0.05$), multiple t-tests with a two-stage linear step-up procedure of Benjamini, Krieger and Yekutieli, with Q = 5%, *$q < 0.05$ (g) and one-way ANOVA, Tukey's multiple comparison test with ***, $P < 0.001$ (h) was used for statistical analysis. Scale bars are shown in each image.

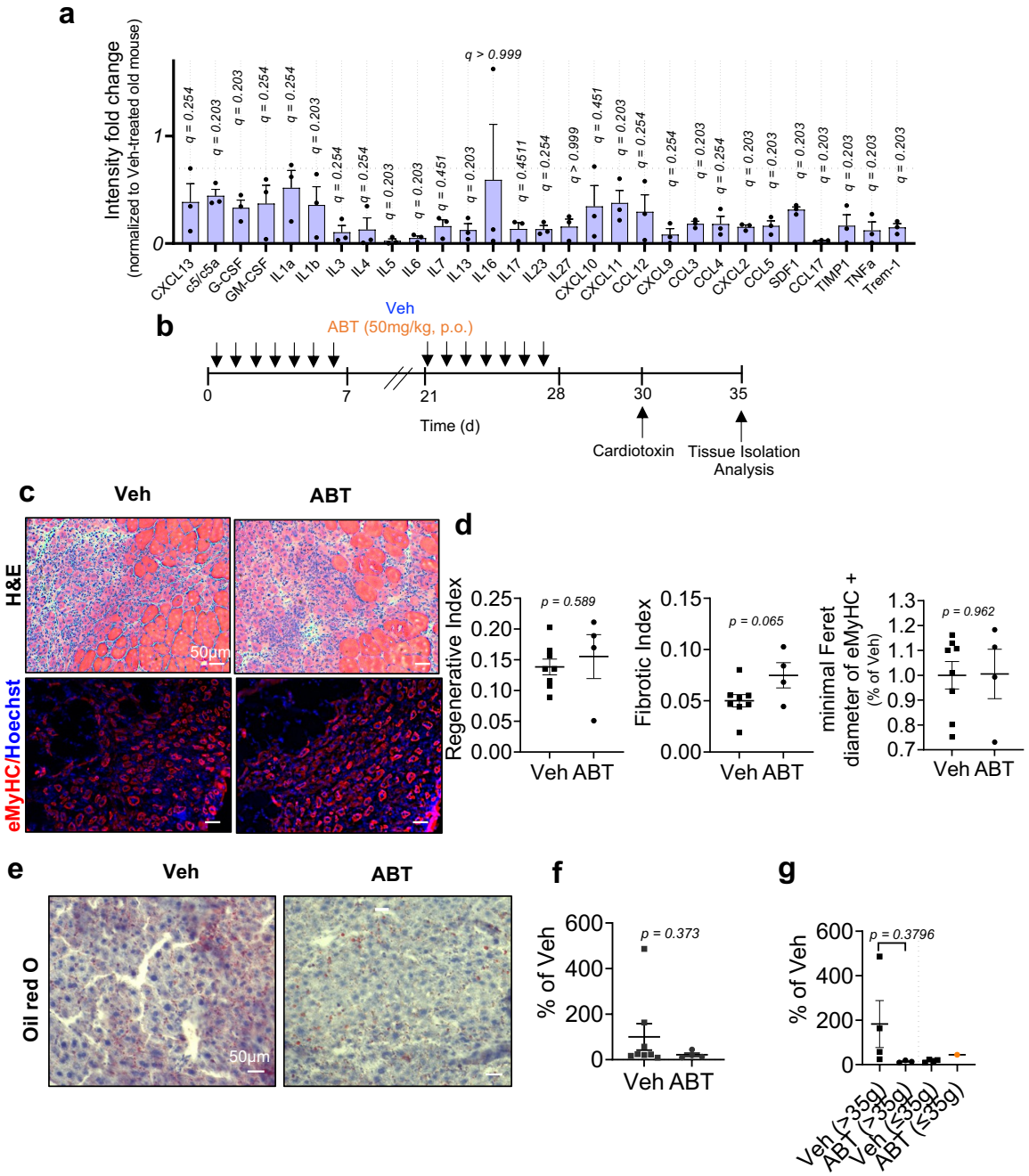
a
Intensity fold change
(normalized to Veh-treated old mouse)
CXCL13
c5/c5a
G-CSF
GM-CSF
IL1a
IL1b
IL3
IL4
IL5
IL6
IL7
IL13
IL16
IL17
IL23
IL27
CXCL10
CXCL11
CCL12
CXCL9
CCL3
CCL4
CXCL2
CCL5
SDF1
CCL17
TIMP1
TNFa
Trem-1
b
Veh
ABT (50mg/kg, p.o.)
Time (d)
Cardiotoxin
Tissue Isolation
Analysis
c
Veh
ABT
H&E
eMyHC/Hoechst
50μm
d
Regenerative Index
Fibrotic Index
minimal Feret diameter of eMyHC + (% of Veh)
p = 0.589
p = 0.065
p = 0.962
Veh ABT
e
Veh
ABT
Oil red O
50μm
f
% of Veh
p = 0.373
Veh ABT
g
% of Veh
p = 0.3796
Veh (>35g)
ABT (>35g)
Veh (≤35g)
ABT (≤35g)

Supplementary Fig 6. Ablation of SnCs in old mice by ABT263 changes circulating SASP factors, does not improve muscle repair and attenuates liver adiposity. (a) Relative expression ratio (< 0.7-fold) of SASP proteins in plasma from ABT263-treated C57BL/6J old mice (ABT) normalized to vehicle treated C57BL/6J old mice (Veh), measured by antibody array. Blood was collected 14 days after the last dose of vehicle or ABT263. (b) Experimental setup for ABT263 treatment for tissue regeneration. (c) Representative images of H&E staining and embryonic myosin heavy chain (eMyHC) immunofluorescence (n = 8 for Veh ; n = 4 for ABT / one image per mice). (d) Quantification of regenerative index (numbers of de novo myofibers/total nuclei per injury site), fibrotic index (areas devoid of white myofibers after H&E staining of the injury site), and the minimal Feret diameter of eMyHC + de novo myofibers, normalized to the Veh sample with the smallest myofibers (n = 8 for Veh; n = 4 for ABT). (e) Representative images of oil red O staining of livers from Veh- or ABT-treated mice (n = 8 for Veh; n = 4 for ABT / 15 images per mice). (f) Quantification of oil red O positive areas per microscopic field, normalized to the mean Veh values, or (g) normalized to body weight (> 35g vs ≤ 35g). The orange dot indicates one ABT mice with a weight less than or equal to 35g, suggesting that Abt might reduce liver adiposity of old mice when mice were overweight (> 35g). Data are means ± s.e.m. of biologically independent samples. Statistical significance was calculated using multiple Mann-Whitney tests with a two-stage linear step-up procedure of Benjamini, Krieger and Yekutieli, with Q = 5% (*, q < 0.05), (a), two-tailed t test (d, f), and 1-way ANOVA followed by Tukey's multiple comparison test (g) with *, P < 0.05. Each data point represents an individual mouse. Scale bars, 50 μm.